PROCEEDINGS

OF THE

THIRD JOINT SYMPOSIUM

ON THE

NATURAL HISTORY AND GEOLOGY OF THE BAHAMAS

Edited by

David Griffing, Mark Kuhlmann and Troy Dexter

ORGANIZER:

Troy A. Dexter

Executive Director
Gerace Research Centre
University of The Bahamas
San Salvador, The Bahamas

2023

ISBN: 978-0-935909-71-5

BOULDER MOVEMENT FROM HURRICANES ALONG THE ROCKY SOUTHERN COAST OF SAN SALVADOR ISLAND, THE BAHAMAS

Tina M. Niemi, Joseph A. Nolan, Stephanie M. Caples, Anna Murray, Tori Rose, Linda Rucker, Jennica Grady, Sara Lamprise, Jessy Zapata, and John D. Rucker

Earth and Environmental Sciences, Division of the Natural and Built Environment
School of Science and Engineering, University of Missouri-Kansas City
Kansas City, MO 64110 U.S.A.

ABSTRACT

Located along the northeastern edge of the Bahamian archipelago, San Salvador Island sees a high frequency of Atlantic hurricanes that track through the Caribbean. This makes the island an excellent location for studying geomorphological processes and changes to the coastal environment due to high-energy waves. The focus of this study is to report on monitoring of coastal erosion and boulder movement along the southern rocky coast at the location called the Gulf on San Salvador Island caused by hurricanes that passed within 60 nautical miles of the island during 2011-2019, including Hurricane Irene (2011), Hurricane Joaquin (2015), and Hurricane Matthew (2016). To map the hurricane-related changes in the coastal environment, two aerial imaging techniques were utilized to photograph the boulder field at the Gulf. Aerial imagery was collected using a kite-mounted camera in June 2015 and March 2016, and using an uncrewed aerial vehicle in March 2016-2018 and June 2016, 2017, and 2019. All data were processed using Agisoft Metashape to render both a high-resolution digital orthophoto mosaic image and a georeferenced digital elevation model. Additionally, ground-based photographic and orientation data for boulder location, imbrication, and beach conditions were collected. The high-resolution, low-altitude imagery allowed us to map the boulder field and calculate boulder movement by matching erosion scars to boulder position, and boulder size to position. Boulders of the Pleistocene fossil reef that are exposed along the wave-cut platform at low tide have been transported up the cliff and inland in storm events based on boulder identification. Coastal reentrants along a rocky island cliff face are the location of coves where wave action is focused, and thus increase the potential to lift boulders. Coastline retreats where cliffs collapse downward are located along these coves and provide large boulders which are available for transport upward. These coves become the staging ground for boulders to be elevated in extreme storm events. Our data show that the coves have a greater storm surge height and transport boulders farther landward. The pronounced landward movement of the entire boulder field during Joaquin is likely due to wave heights as big as 14 m that were caused by the unique intensity, storm track direction from the south with the eyewall passing directly over the island, and long duration of the storm surge.

INTRODUCTION

As the number of annual extreme weather events increases and triggers natural disasters, there is growing data to indicate that the increase in global temperature plays a significant role (UNDRR, 2020). Over the past 150 years, North Atlantic hurricanes may not be getting more frequent (Vecchi *et al.* 2021), but major tropical cyclones since 1980 are getting stronger, intensify faster, and cause more precipitation on landfall as they decay slower (e.g., Bhatia *et al*. 2019; Kossin *et al.* 2020; Li and Chakraborty, 2020). This is of particular consideration to small island nations in the tropics that reside at low elevations and are vulnerable to hurricane storm surge and

inundation (Oppenheimer *et al.* 2019). One country that is notably at risk for hurricane damage is The Bahamas. The Bahamas is a country in the Caribbean that includes over 3000 low-lying islands and cays north and northwest of Cuba and Hispaniola, respectively, and southeast of Florida. It lies along the path of most North Atlantic hurricane storm trajectories. Assessing the effects of past hurricanes in The Bahamas can help inform strategies for mitigation and resilience for all small island nations.

In this study, we report on monitoring the effects of hurricanes on San Salvador Island in The Bahamas over the period between 2012 and 2018. San Salvador is an isolated, small carbonate island located on the eastern or windward side of the Bahamian archipelago (Figure 1). It is surrounded by deep Atlantic Ocean waters, which may play a role in the pattern of hurricane damage on the island. Because the Gerace Research Centre (now the Gerace Research Institute and formerly called the Bahamian Field Station) has been operational on the island since the 1970s, there has been an extensive amount of focused research on San Salvador Island. Attention to documenting the damage and coastal changes caused by tropical storms on the island started with a study posted online by Garver (1996) detailing effects from the category 3 Hurricane Lili (1996), the eyewall of which directly passed over San Salvador. Hurricane Lili traveled from the southwest toward the northeast and had major impacts on the western and southern sides of the island (Garver, 1996).

Statistics of hurricane activity compiled by the Caribbean Hurricane Network (stormcarib.com) indicate that the most active 5-year-perod of storm activity to affect San Salvador during the historical record dating back to 1850 was 1930-1934 when seven tropical storms passed near San Salvador, of which three were major (greater than category 3) hurricanes (Figure 2). However, these same data show that the interval

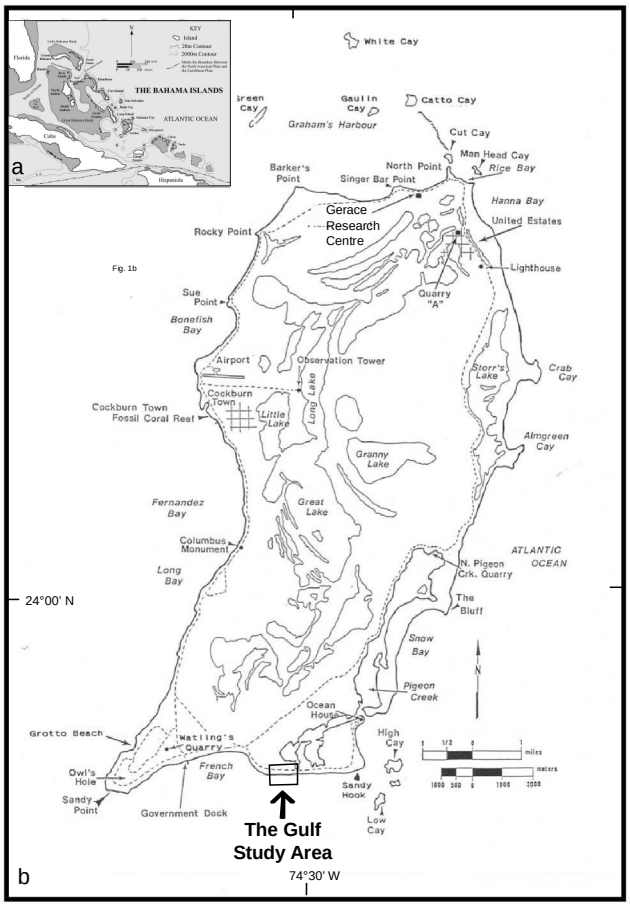

Figure 1. a) San Salvador is a small, isolated carbonate island with deep Atlantic Ocean waters surrounding it located on the eastern, windward side of the Bahamian archipelago. b) The study site called "The Gulf" is located on the southern rocky shore of San Salvador Island. Map after Mylroie and Carew (2010).

1995-1999 was the most active hurricane period with five storms passing within 60 nautical miles (69 mi; 111 km) of the island. These hurricanes included Erin (1995), Bertha (1996), Lili (1996), Dennis (1999), and Floyd (1999). In 1999, the eyewall of the powerful category 4 Hurricane Floyd passed 20-30 nautical miles north of San Salvador. Structural damage from the storm was reported by Gamble *et al.* (2000) and coastal damage was documented by Curran *et al.* (2001). Winds from Hurricane Floyd were most intense from the NW-W thus causing significant coastal erosion on the northern and western sides of the island including erosion of beach sand, formation of beach scarps along the coastal backshore dunes, and rock rubble along beachrock or bedrock strandlines (Curran *et al.* 2001).

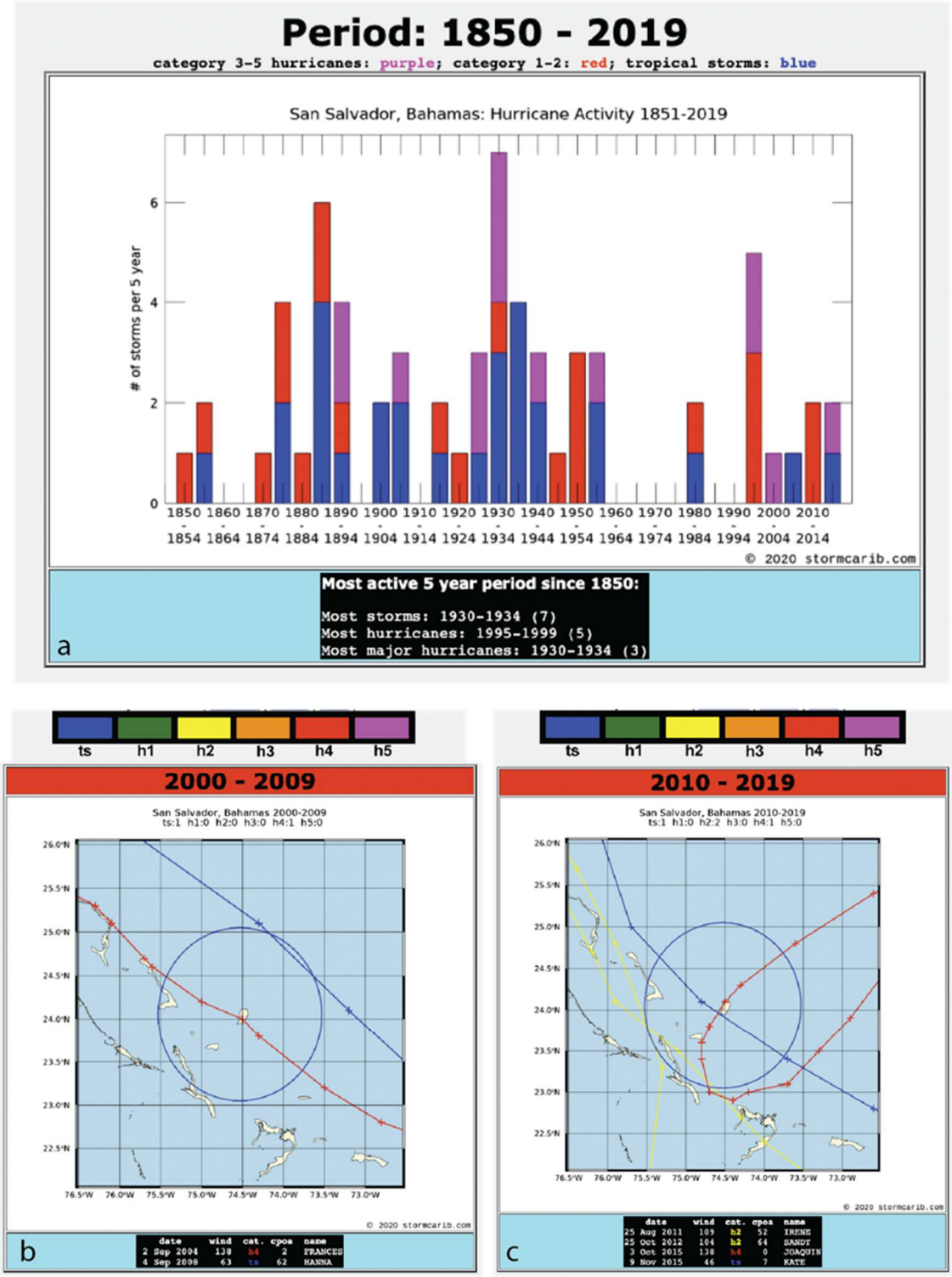

Figure 2. a) Histogram of tropical storms, category 1-2 hurricanes, and major category 3-5 hurricanes in the Bahamas for the time period 1850-2019. The stormiest 5-year period and one with the most major hurricanes was 1930-1934. The most hurricanes of all categories occurred in 1995-1999. b) During the decade 2000-2009, Hurricane Frances (2004) made a direct pass over San Salvador. The only other storm within 60 nautical miles was Tropical Storm Hanna (2008) that passed NW of the island. c) Four tropical cyclones passed close to San Salvador during the interval 2010-2019. The eyewall of category 4 Hurricane Joaquin (2015) tracked directly over the island, followed in the same year one month later by a close pass by Tropical Storm Kate. Hurricane Irene (2011) and Hurricane Sandy (2012) followed a NW track across the Bahamas to the W-SW of San Salvador. (Data source: stormcarib.com).

During the decade between 2000-2009 only two storms passed close to San Salvador, including the direct hit by category 4 Hurricane Frances on September 2, 2004, and Tropical Storm Hanna on September 4, 2008 (Figure 2b). The eyewall of Hurricane Frances passed directly over San Salvador Island from the southeast with a maximum wind speed of 138 mph (Beven 2005) (Figures 2 and 3). Because Gerace Research Centre located on the island provided logistical support for researchers, there are a number of studies that have documented the damage and geological effects from this hurricane (Parnell *et al.* 2004; Niemi *et al.* 2008; McCabe and Niemi 2008; Daehne and Niemi 2010; Dick and Cartright 2011; Curran *et al.* 2012). A storm surge height of greater than 5 m was documented by determining the elevation of the wrack line along the eastern rocky shoreline of the island (Niemi *et al.* 2008; Dick and Cartright 2011). Together these data provide a baseline for continued research on potential hurricane impacts on a small island like San Salvador in The Bahamas.

During the decade between 2010-2019, four tropical storms passed within 60 nautical miles of San Salvador. These included category 2 Hurricane Irene on August 15, 2011, category 2 Hurricane Sandy on October 25, 2012, category 4 Hurricane Joaquin on October 2, 2015, and Tropical Storm Kate on November 9, 2015 (Figure 2c). In this study, we focus on coastal geomorphic changes during the time period of 2012-2018 on San Salvador Island based on our aerial imaging and ground survey data. The goal of our research is to document changes along a rocky shore of the south side of San Salvador Island at a place called the Gulf (Figure 1). High-resolution imagery from kite-mounted and drone cameras over the past decade, along with field observations and data on the direction of boulder imbrication help to illuminate the processes of cliff retreat, boulder formation, and boulder transport along a rocky cliff shoreline during hurricanes. Preliminary results of this study were published in Rose *et al.* (2017) and presented at professional meetings by Preisberga *et al.* (2016), Niemi *et al.* (2017), Caples and Niemi (2018), and Caples *et al.* (2019). Below we outline the parameters for the hurricanes during the period of 2011-2021 that have impacted San Salvador and our data documenting the changes in the coastal environment along the rocky southern coast of the island. These data can help model the potential hazards of cliff retreat, boulder ridge formation and movement, and inundation levels for future hurricanes in The Bahamas and on other small island nations.

Hurricanes Impacting San Salvador Island (2011-2021)

The most significant hurricanes to have impacted San Salvador over the past decade that we have been collecting data at the Gulf site include Hurricane Irene (2011), Hurricane Joaquin (2015), and Hurricane Matthew (2016). Below we summarize the meteorological history and storm tracks of these hurricanes. We also describe subsequent powerful and destructive hurricanes that impacted The Bahamas during the time period 2017-2020.

In 2011, Hurricane Irene (August 21-29) brought strong winds and a storm surge to San Salvador Island. The storm traveled north of Hispaniola on a northwest trajectory and intensified into a category 3 cyclone as the eyewall passed between Mayaguana and Grand Inagua in The Bahamas (Avila and Cangialosi 2011). The hurricane shifted toward the N-NW south of San Salvador as the eye passed over Eleuthera and the winds weakened to category 2 on August 25 as it passed Abaco Island. The diameter of Hurricane Irene was larger than normal size (Avila and Cangialosi 2011).

Hurricane Joaquin was the "strongest October hurricane known to have affected The Bahamas since 1866" (Berg 2016, p. 3), but that record was superseded by subsequent cyclones (see below). The hurricane was unusual as it did not originate in the tropics, but at 27°N or about 360 nautical miles northeast of San Salvador and traveled an atypical path southwest toward the central Bahamas (Berg 2016) and was poorly forecast (Miller and Zhang 2019; Nystrom *et al.* 2018). On October 1, 2015, the storm intensified to a category 4 hurricane, then slowed, and abruptly made a clockwise hairpin turn and

traveled northeast. The unusual looping track caused intense winds for 2 days to be focused on the central southeast Bahamas (Berg 2016). The container ship, *SS El Faro*, sank, killing all 33 members of the crew when it lost power north of The Bahamas and east of San Salvador as it traveled into the eye of the hurricane on October 1, 2015. Hurricane Joaquin passed directly over San Salvador Island on October 2, 2015, with wind speeds of 125 mph (~200 kph) approaching the island from the south. Re-analysis of wind, wave, and ocean current data for the location of the *El Faro* conclude that individual wave heights were >10 m (Bell and Kirtman 2021). Wave simulations and hindcasting of sea state models find wave crests that exceeded 14 m (Fedele *et al.* 2017). Sahoo *et al.* (2019) modeled the hydrodynamic response for the Bahamian archipelago and calculated a maximum significant wave height of 15 m and coast currents of 4 m/s. Together these data indicate Hurricane Joaquin created rogue waves and extreme high-energy wave conditions from October 1-2, 2015. Fuhrmann *et al.* (2019) assessed the storm surge and structural damage of Hurricane Joaquin and found that the average storm surge height was 2.6-3.4 m on San Salvador, with the highest wrack line for storm surge measured on the north side of the island at 5.7 m. However, it must be noted that wrackline elevation for storm surge are only accurate when sufficient unimpeded topographic elevation exists along a coast to record the wave run-up height. The paper by Fuhrmann *et al.* (2019) also does not directly address the boulder field movement at the Gulf location on the island.

Although not within 60 nautical miles of San Salvador Island, Hurricane Matthew was a category 5 hurricane that passed north between Hispaniola and Cuba and then traveled northwest along the southern Bahamian archipelago. It crossed over western New Providence Island on October 6, 2016, as a category 4 hurricane (Stewart 2017). Hurricane-force winds, heavy wave action in the storm surge, and intense rainfall caused damage in Nassau and other northern islands in The Bahamas. Most of the central and south Bahamas including San Salvador Island experienced tropical-storm-force winds (Stewart 2017).

Between 2017-2021, no major hurricanes passed close to San Salvador Island in the central-east Bahamas, but the island likely experienced tropical storm conditions due to several major hurricanes that affected the Caribbean. In 2017, two major hurricanes passed near The Bahamas. The catastrophic Hurricane Irma made four category 5 intensity landfalls as it passed the southeastern Bahamas, paralleled the north coast of Cuba and turned northwest to make landfall in the Florida Keys (Cangialosi *et al.* 2021). Hurricane Maria caused major damage as it passed directly over Puerto Rico and then headed north. In 2018, Hurricane Florence was a major hurricane that passed well north of The Bahamas, making landfall in North Carolina (Stewart and Berg, 2019). In 2019, Hurricane Dorian passed north of San Salvador Island. Hurricane Dorian was the strongest hurricane to make landfall in The Bahamas in modern history, leaving over 200 people dead and massive destruction (Avila *et al.* 2020). It made landfall on Great Abaco and Grand Bahama Islands on September 1-2, 2019, as a category 5 hurricane with minimum low pressure of 910 millibars, an estimated wind of 184 mph (296 kph), and an associated storm surge of >6 m which caused catastrophic flooding (Avila *et al.* 2020). The slow movement of Hurricane Dorian over the northwest Bahamas led to high levels of rainfall exacerbating the coastal inundation. Hurricane Isaias (2020) passed southwest of San Salvador with recorded wind speeds of 54 mph (87 kph) (Latto *et al.* 2021). No hurricanes passed through or near The Bahamas in 2021.

STUDY SITE AND METHODS

Our study focuses on the Gulf site located along the southern coast of San Salvador Island where the deep water of the Atlantic Ocean is closest to the island (Figure 1). The wall of the fringe reefs is as close as 25 m offshore. At the Gulf boulder field site, the shallow carbonate platform extends ~50 m offshore and begins a steep drop to the 2000 m isobath at 130 m from the shoreline. The east-west-oriented rocky coastline at the Gulf site extends for about 1.5 km

and forms the boundary of French Bay to the west. To the east lies the accretionary sand ridge complex that forms the southeastern tip of the island known as Sandy Hook (Figure 1).

The shoreline at the Gulf is marked by a cliff that is approximately 3-4 m in height. The late Pleistocene bedrock at the study site that outcrops along the roadcut and along the shoreline cliff face was described as Fieldtrip Stop 14 by Mylroie and Carew (2010). The rocks belong to the Cockburn Town Member of the Grotto Beach Formation (Figure 3). The uppermost exposed bedrock at the Gulf location is a cross-bedded, oolitic calcarenite deposited in a paleo-sand dune (eolianite). It has a thin paleosol at the top and in the roadcut, the bedrock is topographically higher than the surrounding area because the original sand dune morphology is preserved. In places the exposure of the eolianite along the sea cliff has a much thicker upper paleosol that includes brecciated calcarenite and a penetrative mass of rhizoliths that extend to a depth of 3 m in friable calcarenite (Mylroie and Carew 2010). At low tide, the rock unit below the eolianite that is exposed along the modern wave-cut platform belongs to the lower Cockburn Town Member. It is a calcrudite containing cemented fossil coral reef rubble. We made field observations of coastal erosion of the bedrock exposure and boulder movement and deposition along the eroded cliff face, along a ~600-m-long section of the Gulf outcrop from an access point to the intertidal zone that we call "east cove" to the western edge of the boulder field that was mobilized in 2015 (Figures 3-5). Our field

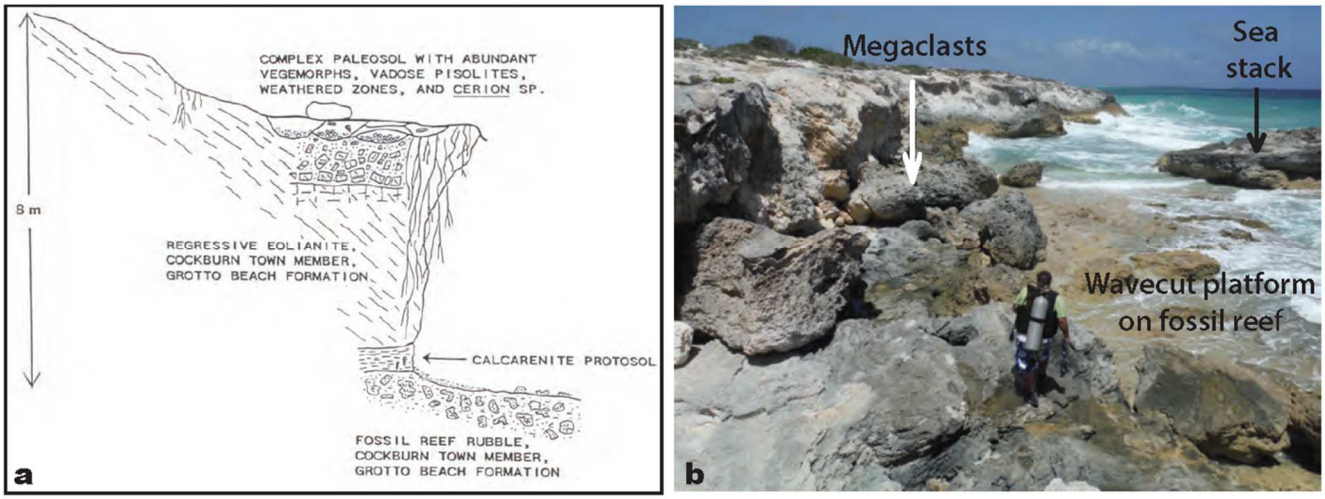

Figure 3. Diagram of the stratigraphy exposed in the cliff and roadcut at the Gulf site showing late Pleistocene fossil coral reef overlain by cross-bedded calcarenite of a fossil sand dune (eolianite). The paleosol on the upper portion of eolianite bedrock contains abundant rhizoliths (vegemorph), is brecciated, and contain red calcrete or terra rosa (from Mylroie and Carew, 2010). b) Photograph from June 2017 of the cliff face at the Gulf looking toward the east showing a sea stack, a wavecut platform developed on the fossil coral reef rumble and the cliff composed of the eolianite. Megaclasts are derived from the collapse of the cliff. Note that the bedrock in the intertidal zone is yellowish in color, the megaclasts have a gray weathered pattern, and the cliff face in the distance is whitish denoting recent erosion.

descriptions began in 2012 (Figure 4) after Hurricane Irene (2011) at east cove and continued each year between 2015-2018. During that time, we also made multiple aerial orthophoto mosaic images of the Gulf cliff edge and boulder field. Below we describe the data collection methods.

In June 2015 before Hurricane Joaquin, aerial photographs were acquired by a camera mounted on a kite that was flown above the Gulf site. Overlapping images were taken using a Canon PowerShot S95 camera with integrated GPS mounted on a Brooxes KAP Delux gondola, carried on an Into-the-Wind Parafoil 10 kite. The gondola uses a servo to trigger the camera mechanically, controlled by an operator using a four channel Futaba 4YF RC transmitter and receiver, operating in the 2.4 GHz range. The camera was stabilized by a three-axis gimbal and

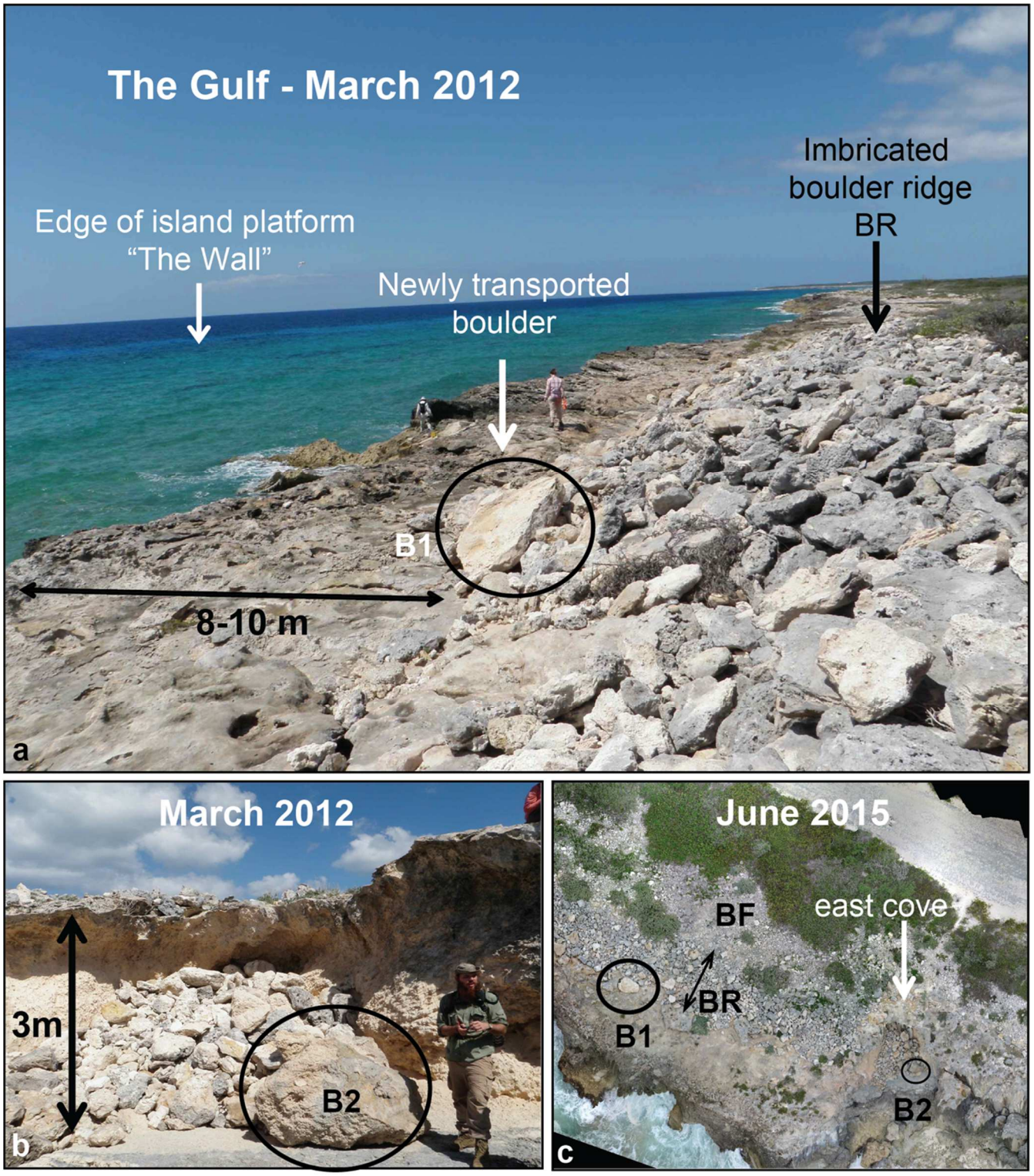

Figure 4. Photographs of the Gulf site prior to Hurricane Joaquin. a) View west along the boulder ridge showing imbricated boulders and freshly transported boulders with light color. Large Boulder B1 can be identified in aerial image shown in Fig. 4c. b) View north of the east cove showing accumulation of boulders at the base of the cliff. Note location of Boulder B2. c) Kite camera aerial photograph of the east cove showing the boulder ridge complex with the ridge (BR) and an inland boulder field (BF). Boulders B1 and B2 from the ground photos are highlighted.

was set to a 3648 x 2736 resolution with ISO 80, shutter speed 1/1000, and a focal ratio of *f*/6.3. Post-Joaquin aerial imagery was collected in 3/2016, 6/2016, 3/2017, 6/2017, 3/2018, and 6/2019. High-resolution aerial orthophotos were collected using a DJI Phantom 3 Advanced uncrewed aerial vehicle (UAV) mounted with a 12 Megapixel, 4K video camera. We preprogrammed flight paths designed to acquire 70% image overlap using a smartphone app designed by Pix4D. In 2018, ground control points (GPC) were placed at strategic locations along the drone flight path and RTK GNSS points were established at each of the GPC using Emlid RS2 antennae receivers. All kite camera and UAV photographic data were processed using Agisoft Metashape to render a high-resolution, digital orthophoto mosaic image. Georeferenced digital elevation models (DEM) were also created by identifying coordinates of stationary points, such as the corner of megaclasts within the imagery field and with GPCs.

Boulder composition, dimensions, and orientation as well as identification of individual boulders at the Gulf boulder field were vital in assessing the wave action and directionality of pre- and post-hurricane boulder movement along the bedrock platform and at the cliff face and base. Prior to Hurricane Joaquin, field data were documented with a tape measure, Brunton compass, and camera. Subsequently, data were collected using a smart phone application, Fieldmove Clino, designed for rapid geologic georeferenced data acquisition. Using the internal compass, GPS, and built-in sensors of the smart phone, the orientation of over 150 individual boulders was acquired, paying special attention to flow directions in the coves and cliff reentrants. This application also allowed the capture of geotagged scaled images of over 30 individual boulders used to verify both size measurements of these boulders, and can potentially serve as good boulder identification markers for any future boulder transport monitoring.

And finally in June 2017, we conducted an underwater scuba dive survey of the subtidal zone at the Gulf site. The purpose of the dive was to inventory the seafloor conditions adjacent to the boulder ridge complex. Two divers entered the ocean at the east cove location and photographed the smooth bedrock, boulders, reef rubble, and patch reefs on the seafloor at various depths along a 30 m transect to water depth of about 20 m.

RESULTS

Coastal Boulder Complex Before Hurricane Joaquin

In March 2012, our ground survey documented the presence of a ridge of imbricated boulders parallel to the rocky southern coast of San Salvador Island at the Gulf site. The boulder ridge is located on top of a bedrock platform that lies above a ~3-m-high sea cliff (Figure 4). Prior to Hurricane Joaquin, the boulder ridge deposit was about 2 m in height and approximately 10 m in width. The seaward edge of the boulder ridge was located 8-10 m landward of the bedrock platform cliff edge and is marked by a few coastal scrub plants. Landward of the boulder ridge was a boulder field that extended about 10-20 m inland (BF in Figure 4). The boulder field was only sparsely vegetated, and the inland limit is shown in Figure 5. The combined boulder ridge and boulder field are defined by Morton *et al.* (2008) as a boulder ridge complex.

The composition of the boulder ridge and boulder field is of locally directed slabs of bedrock and cliff-derived boulders along with smaller offshore cobbles and pebbles. The fresh, unweathered surfaces, i.e., lacking a gray weathering veneer, on several boulders within and at the front of the imbricated boulder ridge in March 2012 (Figure 4), indicated that they had been recently transported by storm waves. One boulder that we measured in 2012 with a long dimension of 2.5 m slid about 50 cm landward in Hurricane Irene exposing unweathered bedrock beneath (Rose *et al.* 2017). Rose *et al.* (2017) report a boulder with a long dimension of 30 cm residing directly on vegetation located 18 m inland along an azimuth of 300°. Multiple white unweathered surfaces on clasts in the boulder ridge and boulder field indicate that individual cobbles and boulders are actively transported across the boulder ridge complex.

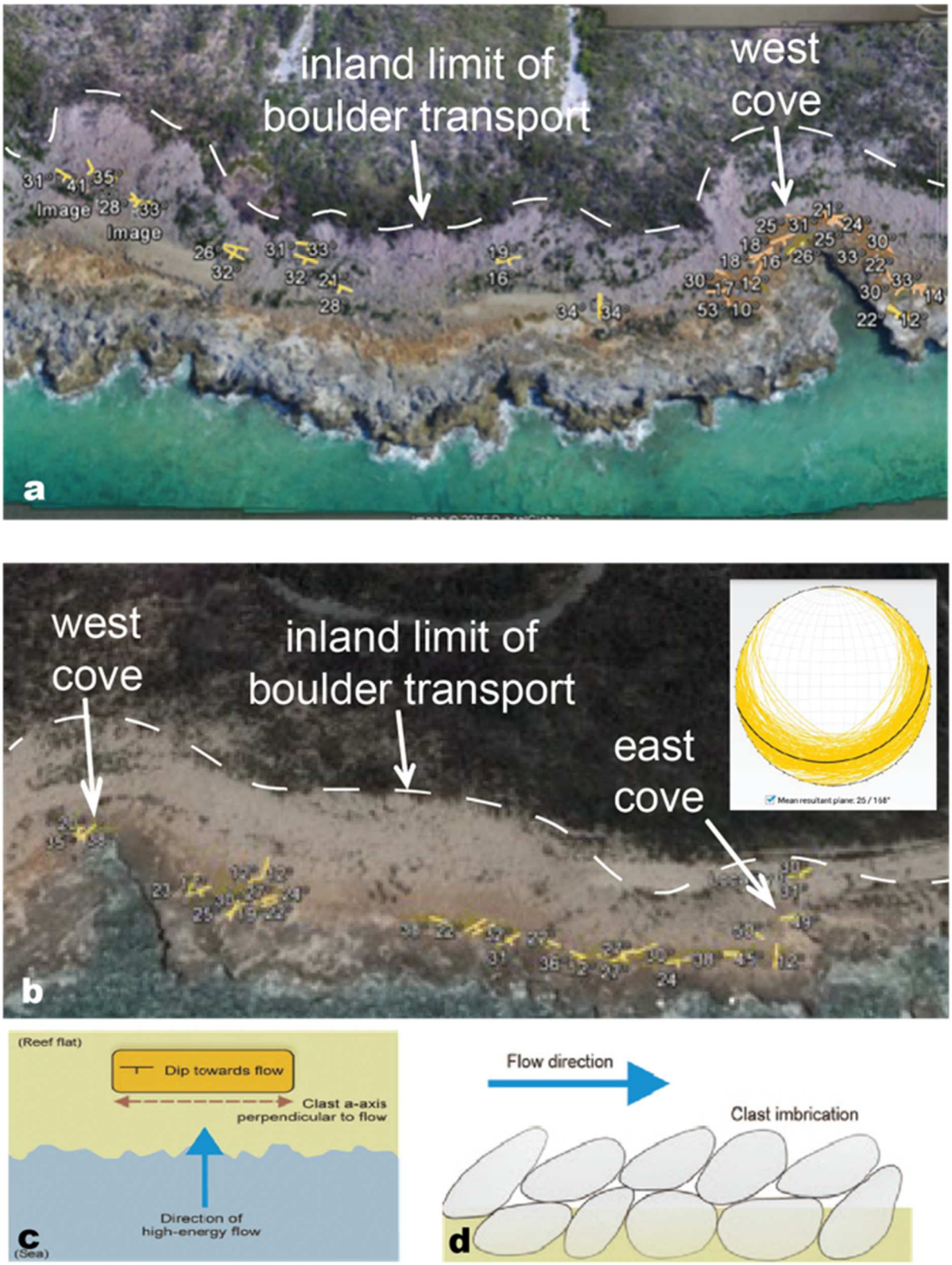

Figure 5. Aerial images marking the inland extent of boulder field transport at the Gulf after Hurricane Joaquin (2015) and shown on the west (a) and east (b) side, respectively, with the west cove in each image. The strike and dip of >100 imbricated boulders is shown along with a stereonet plot of the data collected in March 2018. c) Sketch map shows the long axis of a boulder will align perpendicular to the flow direction and will dip toward the seaward. d) Boulders imbrication in cross section showing clasts stacked and dipping toward the flow direction (Figures 5c and 5d from Terry et al., 2013).

Transport and Deposition of the Boulder Field in Hurricane Joaquin

In the 2015 Hurricane Joaquin, the boulder ridge moved inland, blocked access to the coastal road, and created a larger boulder field that extended ~ 50 m north of the cliff edge. The road running parallel to the shoreline was heavily damaged during Hurricane Joaquin. The boulder field was so thick and wide that the road had to be detoured around it. Coastal shrubs which grew along the backstop of the boulder ridge were uprooted, stripped of foliage, and entrained in the sandy cobbly boulder mobilization. The seaward edge of the boulder field has the largest imbricated clasts and landward edge is a 1.4 m-thick-deposit of poorly sorted cobble breccia. The boulder field can be separated into three lobes or washover fans. Two of these debris lobes are located landward of reentrants or coves that are developed at a high angle to the shoreline cliff face. Because of the poor sorting of most of the boulder deposits in the debris field, imbrication is not pervasive. Although some weathered clasts are present (ones with weathered gray surfaces or reddish with paleosol material), there appear to be an abundance of clasts that have new exposure surfaces without significant evidence of surface weathering. This suggests that the clasts were newly formed from erosional processes. Additionally, erosion of a partially cemented, buried boulder breccia likely provided clasts that moved as debris in the washover fans.

At the seaward edge of the boulder field is a new imbricated boulder ridge composed of large bedrock slabs. The long axis of elongated boulders tends to orient perpendicular to the flow direction and the intermediate axis dips toward the flow direction (e.g. Terry *et al.* 2013). Therefore, measurement of the boulder orientation and imbrication direction can be used to infer the flow direction. Imbricated clasts have a mean dip direction toward an azimuth of 168° (Figure 5). It is clear from our high-resolution imagery time series that high-energy waves routinely sweep above the cliff and have moved cobbles and boulders, but Hurricane Joaquin waves approached from the south-southeast.

Composition and Origin of Clasts

The types of clasts within the boulder field and former imbricated boulder ridge are derived from five main sources and have different transport trajectories. These include: 1) intertidal and subtidal bioclastic material, 2) newly detached and transported boulders from the clifftop, 3) cliff-derived rockfall that is remobilized, 4) boulder ridge breccia, and 5) anthropogenic debris from flotsam and jetsam and local road construction material.

Bioclastic sand, pebbles, and cobbles that are rounded and include coral fragments and shells were deposited around the boulders in the accumulated boulder field. This sediment was also deposited in the hollows or depressions of newly detached slabs (Figure 6). This subtidal sand and gravel are mostly well rounded and sometimes polished showing evidence of prolonged transport within the high-energy surf zone. The beach at the base of the bedrock coastal cliff is a very narrow beach and widens into reentrants or coves along the cliff face. From our observations, sediment of grain sizes smaller than boulders (<25 cm) is not abundant at these beach settings. Our scuba survey conducted in June 2017 in the shallow subtidal zone at the Gulf revealed locations of offshore sediment production and storage. In <10 m water depth, there are subrounded cobbles and boulder and coral fragments in low-lying areas of the wave-cut platform, which may preserve the spur and groove morphology of the underlying fossil reef (Figure 7). In other places, there is a smooth, nearly sediment-free seafloor that appears like an egg carton, with multiple pothole-like depressions scattered across the sea floor. There are a few subrounded boulders in the pothole-like lows (Figure 7). In water depths >12 m, there are active patch reefs that are surrounded by coral rubble and sand. Clasts on the seafloor appear to have a sparse amount of green algae growing on them.

New boulder slabs were clearly dislodged from the top of the bedrock cliff in the storm (Figure 6). The slab thickness of these boulders is controlled by bedding planes of the cross laminated eolianites bedrock. The thickness of the detached slabs is generally 10-30 cm (c-axis). The

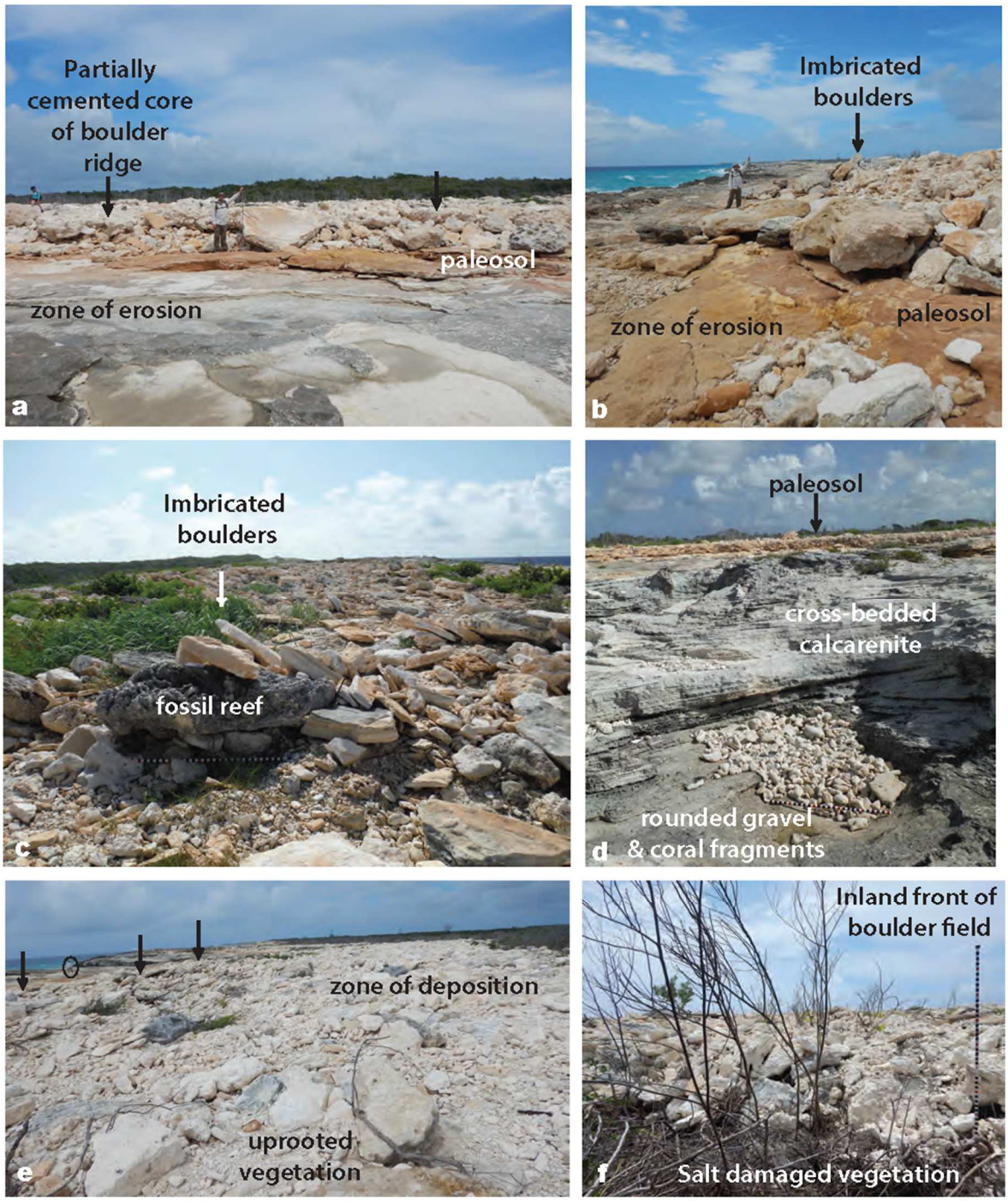

Figure 6. Erosion and deposition of clasts by Hurricane Joaquin at the Gulf site. a) The zone of erosion is characterized by large boulder slabs that have been plucked from the bedrock platform and moved inland to a new ridge. Erosion also exposed the core of the former boulder ridge and the terra rosa paleosol. b) Boulders, some with a long axis >2m, form the edge of a new imbricated boulder ridge inland of the former location. c) A few boulders are of the fossil coral reef and originated at sea level. Newly-formed boulders from the eolianite are imbricated and blade shaped. d) Photograph showing an eroded section through the cross-bedded calcarenite and newly-exposed paleosol and breccia. Rounded clasts and coral fragments have collected in a small cliff reentrant about 1.5 m below the top of the platform. e) Photographic view to the west of the boulder field showing an unsorted sandy gravel deposit that is 40-50 m wide. Arrows point to the shoreward edge of a new imbricated boulder ridge. f) The inland front of the boulder field is about 1.5 thick and terminated in coastal vegetation. Photographs in Fig. 6a, 6b, 6e, 6f are from March 2016, and Fig. 6c and 6d are from June 2016. Pole in photos has markers every 2 cm.

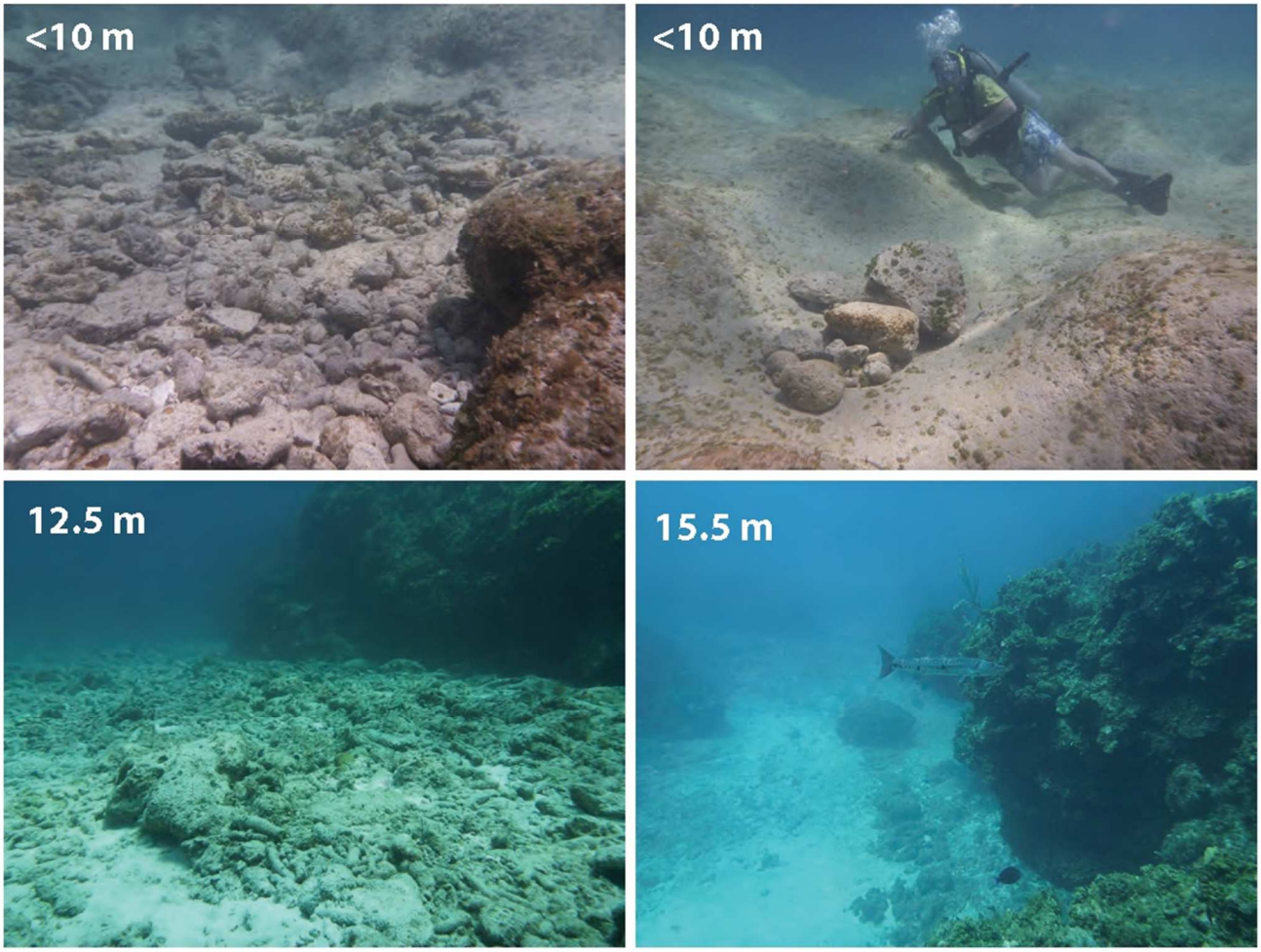

Figure 7. Underwater photographs from June 2017 of the subtidal zone at the east cove of the Gulf site. In <10 m water depth, there are subrounded boulder and coral fragments in low-lying areas of the wavecut platform. Spur and groove topography on the seafloor may be remnants of the underlying fossil reef bedrock. Some areas are completely swept clean of sediment except a few subrounded boulders in pothole-like lows. In water depths >12 m and ~40 m from the intertidal zone, patch reefs are surrounded by sand and coral rubble. Underwater photographs by Jamie R. Stevens, University of Exeter, United Kingdom.

long dimension (a-axis) of these new slabs is on average <1 m and rarely exceeds 2 m. Detachment of new boulders requires more wave energy than in boulder transport (e.g., Terry *et al.* 2013).

Other boulders are derived from cliff erosion and rockfall. Sections of the cliff have collapsed downward to the intertidal zone and have created megaclasts which are boulders with an intermediate b-axis greater than 4.1 m in the modified Udden-Wentworth classification system of Terry and Goff (2014). Cliff-derived Pleistocene calcarenite boulders that are extensively bioturbated with root casts are derived from the uppermost part of the paleodune and are mostly blocky and equant and range from cobbles to boulders with maximum length <2 m in size. Boulders of Pleistocene fossil coral reef from the modern wave-cut platform at sea level are also found, albeit rarely, as clasts with long axes of >1 m.

Erosion of the boulder field in Hurricane Joaquin reveals that the active boulder ridge and boulder field lies above a partially cemented approximately 1.5 m-thick boulder breccia (Figure 6). The boulder breccia deposits were exposed (Figure 6) and provided a large number of clasts for mobilization in the boulder field movement in Hurricane Joaquin.

The Gulf boulder field lies between two topographical highs that mark late Pleistocene

sand dune ridges. When the road was constructed, the bedrock of these high topographic positions was excavated. The road outcrops display excellent crossbedding of sand dunes. It is possible and even probable that part of the clastic accumulation at this site is anthropogenic material deposited during road construction. The deposit is mostly devoid of cultural debris, flotsam and jetsam, that have been prevalent in other hurricane deposits on the island. The storm surge likely elevated the wrack line with the inland run-up and inundation elevation much farther inland than surveyed in this study.

Zone of Erosion

When the boulder ridge was moved inland, it left an exposure of the top of the carbonate bedrock platform showing three zones. This includes an area where new clasts were plucked from the outcrop, exposures of the reddish-colored paleosol, and a cross-section of a partially cemented breccia. New boulder slabs were clearly dislodged from the top of the bedrock cliff in the storm. The slab thickness of these boulders is controlled by bedding planes of the cross laminated eolianites bedrock and is generally 20-30 cm (c-axis). The dimensions of these new slabs are on average 1-2 m and are likely controlled by an orthogonal joint pattern. The long dimension (a-axis) in most cases does not exceed 2 m. In the Zingg particle shape diagram (Zingg 1935), these would be classified as blades or discs. The largest detached boulder slabs appear to have slid. If detachment of new boulders requires more wave energy than in boulder transport (e.g., Terry *et al.* 2013), then this observation is therefore quite significant. The second exposed zone is the base of a reddish-colored paleosol that appears on the top of the bedrock. Mylroie and Carew (2010) call this the terra rossa surface. This is exposed at other locations on the island and is used to identify Pleistocene from Holocene rocks. The new emergence of this 3-4-m-wide paleosol surface suggests that this bedrock area has not been recently or even previously exposed, indicating the uniqueness of Hurricane Joaquin. Some of the cobbles and boulders that have been transported are coated in reddish-colored paleosol suggesting these clasts have not moved for a long time. Finally, the hurricane exposed a stratigraphic section of the boulder ridge and boulder field interior (Figure 6a) that shows the recent cobble and boulders overlie a weakly cemented cobbly boulder breccia. Boulders of breccia are also found in the boulder field.

Monitoring of the cliff face shows that two separate reentrants or coves have formed that we call east cove and west cove (Figure 5). The eastern cove is growing along an azimuth of 325°. East cove was highly eroded during the 2015 Hurricane Joaquin from a perimeter of 31 m and an area of 45 m^2 in 2015, to a perimeter of 46 m and an area of 103 m^2 as observed in March 2016. This erosion occurred through the fracturing of the bedrock cliff surrounding the cove forming into boulders at the cliff base and transported inland (Figure 8). The east cove has continued to grow through jointing and cliff wall collapse as well as wave action. In 2018, the east cove had a 48 m perimeter and was 112 m^2 in area.

Similarly to east cove, west cove is growing along a strike of 325°. Figure 9 shows that there is a conjugate fracture with a strike of 35°. Cliff collapse follows the dominant joint directions and occurred mostly with wave action in Hurricane Matthew (2016). The perimeter and area of the west cove were 152 m and 842 m^2, respectively, in 2014 as observed through satellite imagery. UAV data of the west cove was collected in 2018 and compared to satellite imagery which shows an increase of perimeter to 169 m and the area to 942 m^2. The increase in size is the result of wave activity eroding underlying material creating undercut bedrock beyond the material's angle of repose. Additionally, a significant amount of overhanging bedrock was observed in 2018, which will quickly lengthen and widen the western cove in the near future or during the next hurricane event.

DISCUSSION

The large tsunamis generated in the subduction zone earthquakes in Indonesia in 2004 and Japan in 2011 stimulated an increase in coastal hazards studies from extreme marine

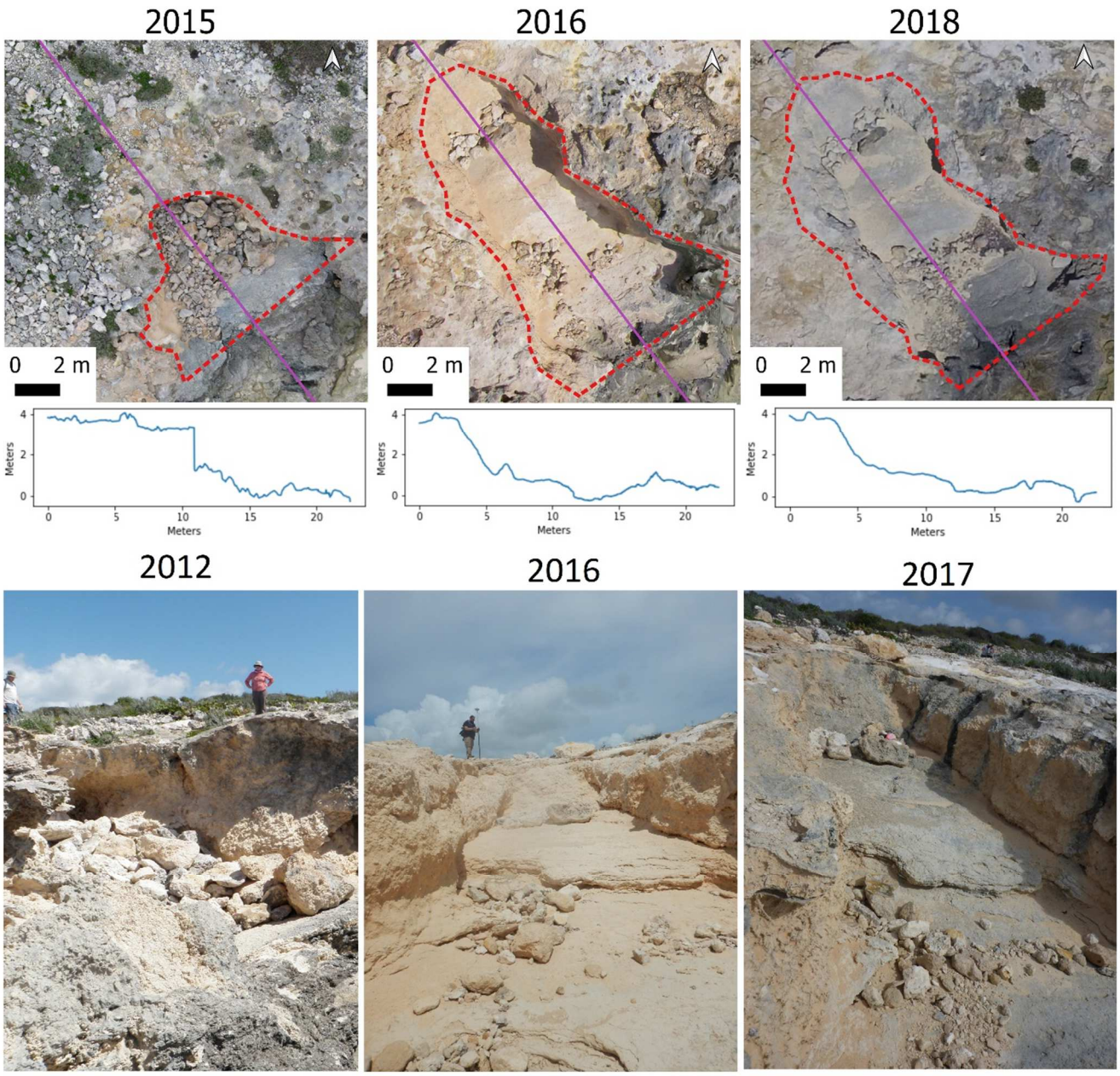

Figure 8. High-resolution kite camera (6/2015) and UAV (2016, 2018) images of the east cove showing the erosion and lengthening of the reentrant (top) and changes to the topographic profiles (middle) before and after Hurricane Joaquin (10/2015). The lower photographs show the boulders accumulated at the cliff base in 2012 (left) and the transport of the boulders up to the platform and erosional elongation of the cove in 2016 (middle). The 2017 photo shows that gray weathering on the bedrock occurs within 2 years. Hurricane Mathew (2016) deposited a buoy and moved boulders. The large boulder at the top of the cliff and the one at the base did not move.

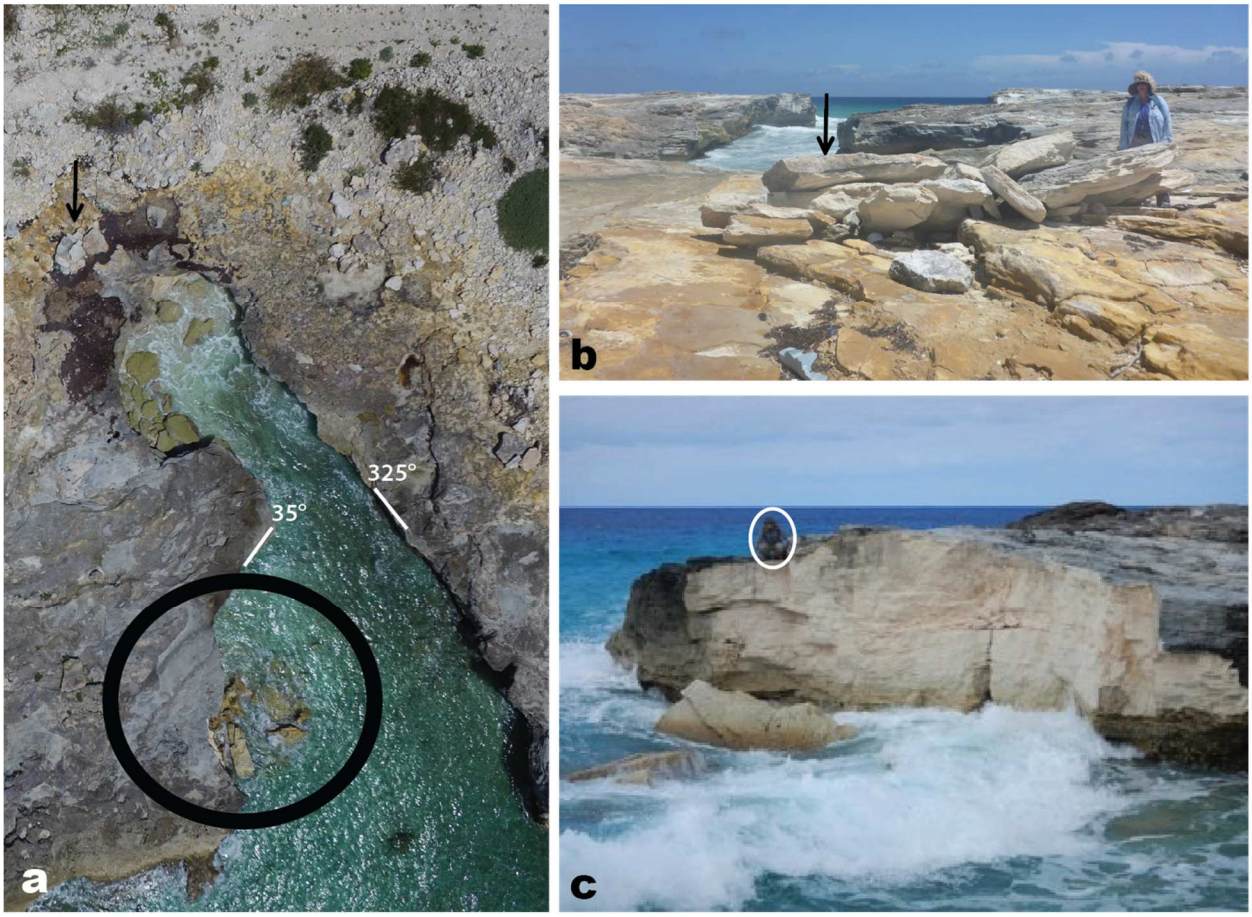

Figure 9. a) A UAV aerial photo of the west cove shows its development along a joint oriented approximately 325°. A second conjugate joint direction is 35°. The arrow points to imbricated boulders deposited in Hurricane Joaquin (2015) and the circle highlights the location of cliff collapse. B) Imbricated boulders deposited at the landward edge of the cove. c) Image of the west side of the cove showing a fresh face of exposed strata and megaclasts in the intertidal zone. The cliff collapsed sometime between June 2017 and March 2018. Oval around a person squatting.

inundation events and has spawned debate as to whether coastal boulder deposits are the result of storm or tsunami waves. Numerous coastal studies around the world published between 2004-2020 interpreted megaboulders to have been transported by tsunamis based on the hydrodynamic equations presented by Nott (2003a, b). The equations use measured boulder dimensions to determine wave height and discern between tsunami and storm waves.

It has become increasingly clear that there are flaws in using the Nott equations as a determination for tsunamic wave transport (Cox *et al.* 2020). Photographic analyses of coastal boulders before and after North Atlantic winter storms along the Irish coast show that boulders as large as 620 tonnes were transported inland over 200 m and to elevations of 29 m above high water (Cox *et al*. 2018). Boulders are larger than ones that are inferred to only have been transported by tsunami waves elsewhere in the world. Furthermore, Cox *et al.* (2019) use scaled wave-tank experiments to model imbricated coastal boulder deposits and showed that storm waves can move megaclasts. Based on linear wave theory and stability analysis, Weiss (2012) concluded that because of the shorter period and longer duration of storm waves that storms have a greater total energy compared to long-period tsunami waves. He further argued that tsunamis should produce unorganized scattered boulder deposits in a dispersed boulder field as was documented in the 2004 Indian Ocean tsunami (Paris *et al.* 2009), the 2009 South Pacific tsunami (Goff and Dominey-Howes 2011), and the 2011 Tohoku tsunami (Goto *et al.* 2012), and that storms would

produce boulder ridges and boulder clusters. Numerical modeling (Weiss and Diplas 2015; Zainali and Weiss 2015; Weiss and Sheremet, 2017) showed that the initiation of large boulder movement is a function of the surface roughness and slope angle. A summary of the debate as to whether storm-transported coastal boulder deposits can be differentiated from tsunami deposits can be found in Dewey *et al.* (2021). In most cases and unlike tsunami waves, high-energy storm waves are unlikely to carry high suspended load (Dewey *et al.* 2021).

On San Salvador, Niemi (2012) and Niemi *et al.* (2015) originally presented the hypothesis that a boulder with a long axis of 4 m and an estimated weight of 14 metric tons on the small island of Green Cay located along the northwestern edge of Graham's Harbour (Figure 1) was transported in a tsunami. However, analyses of aerial imagery before and after Hurricane Frances show that the boulder was transported by wave action in the 2004 storm, and subsequent analyses of our high-resolution aerial imagery helped show how coastal reentrants focus wave action, stage cliff collapse boulders, and result in landward movement of boulders (Niemi 2017; Nolan and Niemi 2020). Boulder movement from the storm surge of Hurricane Frances (2004) was documented at the Gulf site on the south side of San Salvador Island by Niemi *et al.* (2008), and the sliding of bedrock boulder slabs were documented after Hurricane Irene in 2011 (Rose *et al.* 2017).

Our aerial imagery and ground survey data from 2012 and 2015 prior to Hurricane Joaquin revealed the presence of a boulder ridge parallel to the Gulf shoreline on top of a bedrock platform. This site is exposed to high wave energy during most of the year because of the proximity of deep water offshore and the exposed south-southeast windward location. Based on other sites in the Caribbean, linear boulder ridges on top of coastal cliffs and parallel to the shore with imbricated clasts are interpreted to form by transport from high energy waves in successive storms over an extended period of time (Morton *et al.* 2006, 2008; Etienne and Paris 2010). Morton and others (2008) suggested that a coastal boulder ridge is periodically overtopped and makes a boulder field. Together the deposits were defined as a boulder ridge complex (Morton *et al.* 2008). The imbrication of boulders begins because of an obstacle or backstop which can be a steeper slope as demonstrated in wave-tank experiments (Cox *et al.*
2020). Our data show that coastal vegetation may provide the backstop for the development of the boulder ridge. In fact, coastal vegetation may be the predominant factor in the development of boulder ridges. Even a relatively small amount of vegetation can serve as the anchor for a large boulder ridge that builds up after the first layer is caught by the vegetation.

Boulder ridge-complex morphologies and crest elevations are largely controlled by the availability of sediments, clast sizes, and the heights of wave run-ups (Morton *et al.* 2008). Boulders move by sliding, rolling, and saltation, respectively, as the velocity of the water flow increases (e.g. Terry *et al.* 2013). The shape of boulder, whether equidimensional, slabs, or rod-shaped, is an important factor in boulder transport and helps predict whether the boulder will slide and imbricate or roll. The removal of bedrock and formation of boulders through the process of plucking requires higher wave energy than boulder transport (Dewey and Ryan 2017). Hydraulic fracturing plays a dominant role in boulder quarrying from coastal bedrock (Herterich *et al.* 2018).

Structure-from-motion photogrammetry has been used to successfully monitor change in coastal boulder fields, such as along the Irish coast (Nagle-McNaughton and Cox 2020) and in the Philippines (Boesl *et al.* 2019). Sherwood *et al.* (2018) used before and after imagery from the 2016 Hurricane Matthew of a coastal site in Florida and compared it to LIDAR data to determine coastal erosion. Similar to our study, Glumac and Curran (2018, 2019) and Glumac *et al.* (2019) have been monitoring the movement of boulders at various sites including the southern rocky high-energy coastline at the Gulf. They photographed and GPS-located boulders before and after hurricane Joaquin and found that 1-3 ton boulders moved up to 26 m inland. This research

team added UAV aerial imagery in January 2016 (Perlmutter *et al.* 2016) and radio frequency identifiers in 2020 (Lu *et al.* 2020). For our study, we have high-resolution aerial imagery from 2012 and 2015-2018 thus allowing us to also monitor the erosional and depositional processes at the Gulf site.

In general parameters that drive the height of storm surge and wave run-up include the conditions of the storm including atmospheric pressure, wind field size, and wind speed, and other factors include storm trajectory, coastline shape, and offshore bathymetry. On San Salvador the storms that caused the most coastal damage were those that passed directly over the island. Hurricane Frances (2004) moved directly over San Salvador from the southeast to the northwest and Hurricane Irene (2011) passed to the south of island. Hurricane Joaquin (2015) passed over the island from the south, but the clockwise turn in the storm path, two-day duration of intense winds, and rogue waves made the storm unique. The extreme wave energy from Joaquin caused the coastal erosion and boulder transport at the Gulf site. Fuhrmann *et al.* (2019) suggest that the storm surge from Hurricane Joaquin was less than that of Hurricane Frances. Our data show that extraordinary wave heights must have been present locally at the Gulf site.

The coastal configuration of the Gulf site also helps to heighten and focus wave energy as shown in Herterich *et al.* (2018). The shelf is very narrow at the Gulf site and deep water is near to the shore which increases the high wave energy, wave height, and wave run-up. A groove and spur seafloor morphology on the shelf at the Gulf documented in our scuba survey likely further focuses flow and amplifies hydrodynamic forces as has been shown, for example, in an elevated Holocene reef platform in Taiwan (Terry *et al.* 2021). Along the coastal cliff, reentrants and coves also focus wave energy as we documented on Green Cay (Niemi 2017; Nolan and Niemi 2020) and on New Providence Island after Hurricane Matthew in 2016 (Rucker *et al.* 2020). Herterich *et al.* (2018) show bathymetric and topographic lows help focus wave energy and help to hydraulically produce boulders.

Our data from the Gulf show that coves form at locations where the bedrock is weakly cemented with extensive rhizolith formation and along coastal extensional fractures. Cliff retreat processes are controlled by a conjugate joint pattern that trend approximately 35° and 325°. Focused wave energy within the coastal reentrants causes a cove to elongate and widen. The development of a wave-cut notch along the intertidal zone undercuts the cliff. Storm wave action within the cove causes the sidewalls of the cove to collapse. The rockfall at the base of the cliff from the collapse produces megaclasts and boulders. Wave action then reduces the size of the boulders and transports them toward the coves where they collect. Boulders act as an abrasive agent to further grind and erode the end and sides of the cove. Boulders in the cove provide a staging ground for clasts that are then transported to the top of the cliff and inland to the boulder ridge by storm surge and wave run-up bores. Some smaller clasts fill gaps in the boulder ridge and others move farther inland to the boulder field. Within two years newly exposed bedrock in the cove that was enlarged in the Joaquin storm surge has a surface veneer of gray weathering. New boulders identified by the freshly eroded white surface are continuously being added to the coastal boulder deposits at the top of the cliff platform.

CONCLUSIONS

There has been heightened research on investigating coastal boulders and applications for quantification of coastal hazards. Mapping the zone of coast boulder ridges and boulder fields can help to determine the inland extent of inundation and the maximum run-up height. Washover fans, debris aprons, and imbricated boulders are used to determine the direction of transport and the angle of approach of storms. New methods to track boulders and image before and after storm boulder fields help to determine the mechanism for the generation and movement of boulders into staging areas, boulder ridges, and boulder fields and limitations to these movements. One of the major challenges that small, low-lying

island nations face is the determination of the likelihood of a potential extreme marine inundation event and whether existing coastal deposits can be used to back-calculate storm wave energy and run-up parameters.

Coastal boulder deposits accumulate on rocky coastlines with high amounts of wave energy. This is most common when there is a combination of open-ocean exposure and steep topography combining to create boulder supply and high wave heights and storm surge. Waves are amplified by these conditions and can create and transport large clasts as the bedrock of the coastline is broken up. Our aerial imagery shows in 2012 that the boulder ridge and boulder field are actively moving boulders based on the clear white, unweathered appearance of the boulders. Waves from the storm surge of the category 3 Hurricane Joaquin (2015) at the Gulf site transported the previously well-defined, shore-parallel boulder ridge landward, exposed the terra rossa paleosol and the internal structure of a partially cemented boulder breccia, eroded boulder slabs from the coastal bedrock platform, and deposited a new boulder field ~50 m inland of the cliff edge. As confirmed from sea-state modeling of Hurricane Joaquin (Fedele *et al.* 2017; Bell and Kirtman 2021), wave heights may have been in excess of 14 m along at the Gulf site on the southern rocky shore of San Salvador.

ACKNOWLEDGEMENTS

This research was performed under a permit issued by The Bahamas Environment, Science, and Technology Commission to Niemi. We would like to thank Dr. Troy Dexter, director of the Gerace Research Center, and all of the GRC staff for their logistical support. We would also like to acknowledge the help of Jamie R. Stevens in leading the scuba dive survey at the Gulf site in 2017 and for underwater photography. Caples and Zapata were funded through University of Missouri-Kansas City's SEARCH and SUROP undergraduate research grants.

LITERATURE CITED

Avila, L., and Cangialosi, J., 2011, Hurricane Irene, 21–28 August 2011: *NOAA National Hurricane Center Tropical Cyclone Report*, AL092011, 36 p.

Avila, L., Stewart, S.R., Berg, R., and Hagen, A.B., 2020, Hurricane Dorian, 24 August-September 2019: *NOAA National Hurricane Center Tropical Cyclone Report*, AL052019, 74 p.

Bell, R., and Kirtman, B., 2021, Extreme environmental forcing on the container ship SS El Faro: *Journal of Operational Oceanography*, v. 14, no. 2, p. 98-113.

Berg, R., 2016, Hurricane Joaquin - 28 September - 7 October 2015: *NOAA National Hurricane Center Tropical Cyclone Report*, AL112015, 25 p.

Beven II, J.L., 2005, Hurricane Frances 25 August – 8 September 2004: *NOAA National Hurricane Center Tropical Cyclone Report*, AL062004, 30 p.

Bhatia, K.T., Vecchi, G., Knutson, T.R., Murakami, H., Kossin, J., Dixon, K.W., and Whitlock, C.E., 2019, Recent increases in tropical cyclone intensification rates. *Nature Communications*, 10, Article number: 3942.

Boesl, F., Engel, M., Eco, R.C., Galang, J.B., Gonzalo, L.A., Llanes, F., Quiz, Ev., and Brückner, H., 2019, Digital mapping of coastal boulders—high resolution data acquisition to infer past and recent transport dynamics: *Sedimentology*, doi: 10.1111/sed.12578.

Cangialosi, J.P., Latto, A.S., and Berg, R., 2021, Hurricane Irma – 30 August - 12 September 2017: *NOAA National Hurricane Center Tropical Cyclone Report*, AL112017, 111 p.

Caples, S.M. and Niemi, T.M., 2018, Comparing Hurricane Matthew (2016) and Hurricane Joaquin (2015) boulder transport on San Salvador Island, The Bahamas: *Geological Society of America Abstracts with Programs*. Vol. 50, No. 4, doi: 10.1130/abs/2018NC-313107

Caples, S.M., Niemi, T.M., Nolan, J., Rucker, J., Moore, L., and Grady, J., 2019, High-resolution imagery of boulder field movement in Hurricanes Irene (2011), Joaquin (2015), and Matthew (2016) on San Salvador, The Bahamas: *3rd Joint Symposium on the Natural History and Geology of The Bahamas*, Gerace Research Centre, San Salvador, The Bahamas, June 8-12, 2019.

Cox, R., Ardhuin, F., Dias, F., Autret, R., Beisiegel, N., Earlie, C.S., Herterich, J.G., Kennedy, A., Paris, R., Raby, A., Schmitt, P., and Weiss, R., 2020, Systematic review shows that work done by storm waves can be misinterpreted as tsunami-related because commonly used hydrodynamic equations are flawed: *Frontiers in Marine Science*, doi: 10.2289/fmars.2020.00004.

Cox, R., O'Boyle, L., and Cytrynbaum, J., 2019, Imbricated coastal boulder deposits are formed by storm waves, and can preserve a long-term storminess record: *Scientific Reports*, doi.org/10.1038/s41598-019-47254-w.

Cox, R., Jahn, K.L., Watkins, O.G., and Cox, P., 2018, Extraordinary boulder transport by storm waves (west of Ireland, winter 2013-2014), and criteria for analysing coastal boulder deposits: *Earth-Science Reviews*, v. 177, p. 623-636.

Curran, H.A., Schultz-Baer, M., Durkin, K., and Glumac, B., 2012, Recovery of carbonate sand beaches on San Salvador island, Bahamas from damage by Hurricane Frances (2004), *in* Gamble, D.W., and Kindler, P., eds., *Proceedings of the 15th Conference on the Geology of the Bahamas and Other Carbonate Islands*: San Salvador, Bahamas, Gerace Research Centre, p. 1-14.

Curran, H.A., Delano, P., White, B., and Barret, M., 2001, Coastal effects of Hurricane Floyd on San Salvador Island, Bahamas, *in* Greenstein, B.J., and Carney, C.K., eds., *Proceedings of the 10th Conference on the Geology of the Bahamas and Other Carbonate Islands*: San Salvador, Bahamas, Gerace Research Centre, p. 1-12.

Daehne, A., and Niemi, T.M., 2010, Changes in vegetation and coastal morphology on San Salvador, Bahamas following Hurricane Frances in 2004, *in* Siewers F., and Martin, J.B., eds., *Proceedings of the 14th Conference on the Geology of the Bahamas and Other Carbonate Islands*: San Salvador, Bahamas, Gerace Research Centre, p. 42-52.

Dewey, J.F., Goff, J., and Ryan, P.D., 2021, The origins of marine and non-marine boulder deposits: a brief review: *Natural Hazards*, v. 109, p. 1981-2002.

Dewey, J.F., and Ryan, P.D., 2017, Storm, rogue wave, or tsunami origin for megaclast deposits in western Ireland and North Island, New Zealand?: *Proceedings of the National Academy of Sciences*, www.pnas.org/cgi/doi/10.1073/pnas.1713233114.

Dick, J.C., and Cartright, G.R., 2011, Assessment of the Hurricane Frances storm surge on San Salvador, *in* Baxter, J.A., and Cole, E.S., eds., *Proceedings of the 13th Conference on the Natural History of the Bahamas and Other Carbonate Islands*: San Salvador, Bahamas, Gerace Research Centre, p. 59-63.

Etienne, S., and Paris, 2010, Boulder accumulations related to storms on the south coast of the Reykjanes Peninsula (Iceland): *Geomorphology*, v. 114, p. 55-70.

Fedele, F., Lugni, C., and Chawla, A., 2017, The sinking of the El Faro: Predicting real world rogue waves during Hurricane Joaquin: *Scientific Reports*, v. 7, no. 1, doi:10.1038/s41598-017-11505-5.

Fuhrmann, C.M., Wood, K.M., and Rodgers, J.C., Assessment of storm surge and structural damage on San Salvador Island, Bahamas, associated with Hurricane Joaquin (2015): *Natural Hazards*, v. 99, p. 913-930.

Gamble, D. W., Brown, M. E., Parnell, D., Brommer, D., and Dixon, P. G., 2000, Lessons learned from Hurricane Floyd damage on San Salvador: *Bahamas Journal of Science*, v. 8, p. 25-31.

Garver, J., 1996, Some effects of Hurricane Lili (Oct 1996) on San Salvador Island, Bahamas. Retrieved 13 April 2022 from https://idol.union.edu/garverj/Geo35/hurricane/Damage.htm.

Glumac, B., Miguel, U., and Curran, A.H., 2019a, New advances in long-term monitoring of storm-deposited boulder ridges along rocky shorelines of San Salvador Island, Bahamas: *3rd Joint Symposium on the Natural History and Geology of The Bahamas*, Gerace Research Centre, San Salvador, The Bahamas, June 8-12, 2019.

Glumac, B., and Curran, A.H., 2019b, Generation and transport of large rock boulders by storm wavs along the high-energy southern coast of San Salvador Island, Bahamas: *3rd Joint Symposium on the Natural History and Geology of The Bahamas*, Gerace Research Centre, San Salvador, The Bahamas, June 8-12, 2019.

Glumac, B., and Curran, A., 2018, Documenting the generation and transport of large rock boulders by storm waves along the high-energy southern coast of San Salvador Island, Bahamas: American Geophysical Union, Fall Meeting 2018, abstract #EP23C-2296.

Goff, J., and Dominey-Howes, D., The 2009 South Pacific Tsunami: Earth-Science Revies, v. 107, doi:10.1016/j.earscirev.2011.03.006.

Goto, K., Sugawara, D., Ikerma, S., Miyagi, T., 2012, Sedimentary processes associated with sand and boulder deposits formed by the 2011 Tohoku-oki tsunami at Sabusawa Island, Japan: *Sedimentary Geology*, v. 282, p. 188-198.

Herterich, J.G., Cox, R., and Dais, F., 2018, How does wave impact generate large boulders? Modeling hydraulic fracture of cliffs and shore platforms: *Marine Geology*, doi: 10.1016/j.margeo.2018.01.00.

Kossin, J.P., Knapp, K.R., Olander, T.L., Velden, C.S., 2020, Global increase in major tropical cyclone exceedance probability over the past four decades: *Proceedings of the National Academy of Sciences*, v. 117, no. 22, p. 11,975-11,980.

Latto, A., Hagen, A., and Berg, R., 2021, Hurricane Isaias – 20 July - 4 August 2010: *NOAA National Hurricane Center Tropical Cyclone Report*, AL092020, 84 p.

Li, L., and Chakraborty, P., 2020, Slower decay of landfalling hurricanes in a warming world: *Nature*, v. 587, p. 230-234.

Lu, K., Mugabekazi, V.R., Pharris, G., Atkinson, E., Fischer, N., Gahwagy, R., Holt, C., Harnishch, E., Glumac, B., and Curran, H.A., 2020, Application of drones in monitoring limestone boulder generation and transport by storm waves along rocky shorelines of San Salvador Island, Bahamas: *Geological Society of America Abstracts with Programs*, v. 52, no. 6, doi: 10.1130/abs/2020AM-353424.

McCabe, J.M. and Niemi, T.M., 2008, The 2004 Hurricane Frances overwash deposition in Salt Pond, San Salvador, The Bahamas, *in* Park, L.E., and Freile, F., eds., *Proceedings*

of the 13th Conference on the Geology of the Bahamas and Other Carbonate Islands: San Salvador, Bahamas, Gerace Research Centre, p. 25-41.

Miller, W., and Zhang, D.-L., 2019, Understanding the unusual looping track of Hurricane Joaquin (2015) and its forecast errors: *Monthly Weather Review*, doi:10.1175/MWR-D-18-0331.1.

Morton, R.A., Richmond, B.M., Jaffe, B.E., and Gelfenbaum, G., 2006, Reconnaissance investigation of Caribbean extreme wave deposits—Preliminary observations, interpretations, and research directions: U.S. Geological Survey, Open-File Report 2006-1293, 41 p.

Morton, R.A., Richmond, B.M., Jaffe, B.E., and Gelfenbaum, G., 2008, Coarse-clast ridge complexes of the Caribbean: A preliminary basis for distinguishing tsunami and storm-wave origins: *Journal of Sedimentary Research*, v. 78, p. 624-637.

Mylorie, J.D., and Carew, J.L, 2010, Field guide to the geology and karst geomorphology of San Salvador island. [Publisher unknown], USA.

Nagle-McNaughton, T., and Cox, R., 2020, Measuring change using quantitative differencing of repeat structure-from-motion photogrammetry: The effect of storms on coastal boulder deposits: *Remote Sensing*, v. 12, no. 42; doi:10.3390/rs12010042.

Niemi, T.M., 2012, Tsunami boulders, storm deposits, and sea level variation on San Salvador in the Bahamas: *16th Conference on the Geology of The Bahamas and Other Carbonate Islands*, Gerace Research Centre, San Salvador, The Bahamas, June 14-18, 2012.

Niemi, T.M., Grady, J., and Billingsley, A., 2015, Evidence of a possible tsunami on San Salvador Island, The Bahamas: *1st Joint Symposium on the Natural History and Geology of The Bahamas*, Gerace Research Centre, San Salvador, The Bahamas, June 12-17, 2015.

Niemi, T.M., 2017, Large boulders on Green Cay, San Salvador Island, The Bahamas, in *Proceedings of the 1st Joint Symposium on the Natural History and Geology of The Bahamas*, Landry, C., and Florea, L., (eds.), Gerace Research Centre, San Salvador, The Bahamas, p. 121-129.

Niemi, T.M., Preisberga, A., Rucker, J.D., Nolan, J., and Rose, T.L., 2017, Mapping coastal boulders with an unmanned aerial vehicle (UAV): *Proceedings of the 2nd Joint Symposium on the Natural History and Geology of The Bahamas*, Gerace Research Centre, San Salvador, The Bahamas, June 8-12, 2017.

Niemi, T.M., Thomason, J.C., McCabe, J.M., and Daehne, A., 2008, Impact of the September 2, 2004 Hurricane Frances on the coastal environment of San Salvador island, The Bahamas, *in* Park, L.E., and Freile, D., eds., *Proceedings of the 13th Conference on the Geology of the Bahamas and Other Carbonate Islands*: San Salvador, Bahamas, Gerace Research Centre, p. 42-62.

Nolan, J., and Niemi, T.M., 2020, Detection of boulder transport via storm surge using drone imagery on Green Cay, San Salvador, The Bahamas: *Proceedings of the 2nd Joint Symposium on the Natural History and Geology of The Bahamas*, Niemi, T.M. and Sullivan Sealey, K., (eds.), Gerace Research Centre, San Salvador, The Bahamas, p. 94-102.

Nott, J., 2003a, Waves, coastal boulder deposits and the importance of the pre-transport setting: *Earth and Planetary Science Letters*, v. 210, p. 269-276.

Nott, J., 2003b, Tsunami or storm waves?—Determining the origin of a spectacular field of wave emplaced boulders using numerical storm surge and wave models and hydrodynamic transport equations: *Journal of Coastal Research*, v. 19, p. 348-356.

Nystrom, R.G., Zhang, F., Munsell, E.B., Braun, S.A., Sippel, J.A., Weng, Y., and Emanuel, K., 2018, Predictability and dynamics of Hurricane Joaquin (2015) explored through convection-permitting ensemble sensitivity experiments: *Journal of the Atmospheric Sciences*, v. 75, no. 2, p. 401-424.

Oppenheimer, M., B.C. Glavovic , J. Hinkel, R. van de Wal, A.K. Magnan, A. Abd-Elgawad, R. Cai, M. Cifuentes-Jara, R.M. DeConto, T. Ghosh, J. Hay, F. Isla, B. Marzeion, B. Meyssignac, and Z. Sebesvari, 2019, Sea level rise and implications for low-lying islands, coasts and communities. In: *IPCC Special Report on the Ocean and Cryosphere in a Changing Climate* [H.-O. Pörtner, D.C. Roberts, V. Masson-Delmotte, P. Zhai, M. Tignor, E. Poloczanska, K. Mintenbeck, A. Alegría, M. Nicolai, A. Okem, J. Petzold, B. Rama, N.M. Weyer (eds.)]. Cambridge University Press, Cambridge, UK and New York, NY, USA, pp. 321–445. doi.org/10.1017/9781009157964.006.

Paris, R., Wassmer, P., Sartohadi, J., Lavigne, F., Barthomeuf, B., Desgages, E., et al., 2009, Tsunamis as geomorphic crises: lessons from the December 26, 2004 tsunami in Lhok Nga, West Banda Aceh (Sumatra, Indonesia): *Geomorphology*, v. 104, p. 59–72.

Parnell, D.B., Brommer, D., Dixon, P.G., Brown, M.E., and Gamble, D.W., 2004, A survey of Hurricane Frances damage on San Salvador: *Bahamas Journal of Science*, v. 12, p. 2-6.

Perlmutter, E., Caris, J., Widstrand, A., Curran, H.A., and Glumac, B., 2016, Drone use in rapid assessment of Hurricane Joaquin coastal impact on San Salvador Island, Bahamas: *Geological Society of America Abstracts with Programs.* v. 48, no. 7, doi: 10.1130/abs/2016AM-282290

Preisberga, A., Niemi, T.M., Rucker, J., Nolan, J., Grady, J., and Lamprise, S., 2016, High-resolution UAV imaging and mapping of coastal erosion and boulder movement produced by the 2015 Hurricane Joaquin on San Salvador, The Bahamas: *Geological Society of America Abstracts with Programs.* v. 48, no. 7, doi: 10.1130/abs/2016AM-287520.

Rose, T.L., Moore, L., Preisberga, A., and Niemi, T.M., 2017, Monitoring changes in the coastal environment on San Salvador Island using beach profiling, real-time kinematic GPS surveys, and kite imagery, in *Proceedings of the 1st Joint Symposium on the Natural History and Geology of The Bahamas*, Landry, C., and Florea, L. (eds.), Gerace Research Centre, San Salvador, The Bahamas, p. 131-141.

Rucker, J.D., Niemi, T.M., Nolan, J., and Rose, T., 2020, Aerial photography of coastal erosion and large boulder transport from Hurricane Matthew along Clifton Beach, New Providence Island, The Bahamas, in *Proceedings of the 2nd Joint Symposium on the Natural History and Geology of The Bahamas*, Niemi, T.M. and Sullivan Sealey, K., and (eds.), Gerace Research Centre, San Salvador, The Bahamas, p. 83-93.

Sahoo, S., Jose, F., and Bhaskaran, P.K., 2019, Hydrodynamic response of Bahamas archipelago to storm surge and hurricane generated waves—A case study for Hurricane Joaquin: *Ocean Engineering*, v. 184, p. 227-238.

Sherwood, C.R., Warrick, J.A., Hill, A.D., Ritchie, A.C., Andrews, B.D., and Plant, N.G., 2018, Rapid, remote assessment of Hurricane Matthew impacts using four-dimensional structure-from-motion

photogrammetry: *Journal of Coastal Research*, v. 34, no. 6, p. 1303-1316.

Stewart, S.R., 2017, Hurricane Matthew – 28 September – 9 October 2016: *NOAA National Hurricane Center Tropical Cyclone Report*, AL142016, 82 p.

Stewart, S.R., and Berg, R., 2019, Hurricane Florence – 31 August – 17 September 2018: *NOAA National Hurricane Center Tropical Cyclone Report*, AL062018, 98 p.

Terry, J.P., Lau, A.Y.A., and Etienne, S., 2013, *Reef-Platform Coral Boulders: Evidence for High-Energy Marine Inundation Events on Tropical Coastlines*: Springer Briefs in Earth Sciences, Heidelberg, Germany, 105 p.

Terry, J.P., and Goff, J., 2014, Megaclasts: proposed revised nomenclature at the coarse end of the Udden-Wentworth grain-size scale for sedimentary particles: *Journal of Sedimentary Research*, v. 84, p. 192-197.

Terry, J.P., Lau, A.Y.A, Nguyen, K.A., Liou, Y.-A., and Switzer, A.D., 2021, Clustered, stacked and imbricated large coastal rock clasts on Ludao Island, Southeast Taiwan, and their application to palaeotyphoon intensity assessment: *Frontiers in Earth Science*, doi:10.3389/feart.2021.792369.

UNDRR, 2020, *Human Cost of Disasters: An Overview of the Last 20 Years (2000-2019)*: *U*nited Nations Office of Disaster Risk Reduction, 30 p.

Vecchi, G.A., Landsea, Zhang, W., Villarini, G., and Knutson, T., 2021, Changes in Atlantic major hurricane frequency since the late-19th century: *Nature Communications*, v. 12, Article number: 4054.

Weiss, R., 2012, The mystery of boulders moved by tsunamis and storms: *Marine Geology*, v. 295-298, p. 28-33.

Weiss, R., and Diplas, P., 2015, Untangling boulder dislodgement in storms and tsunamis: Is it possible with simple theories?: *Geochemistry, Geophysics, Geosystems*, v. 16, p. 890–898. doi: 10.1002/2014GC005682.

Weiss, R., and Sheremet, A., 2017, Toward a new paradigm for boulder dislodgement during storms: *Geochemistry, Geophysics, Geosystems*, v. 18, p. 2717–2726. doi: 10.1002/2017GC006926

Zainali, A., and Weiss, R., 2015, Boulder dislodgement and transport by solitary waves: insights from three-dimensional numerical simulations: *Geophysical Research Letters*, v. 42, p. 4490–4497, doi: 10.1002/2015GL063712.

Zingg, T., 1935, Beitrag zur Schotteranalyse: *Schweizeriscke Mineralogische und Petrologische Mitteilungen*, v. 15, p. 39–140.